Design for Manufacturing Tool for Automated Fiber Placement Structures – Verification and Validation

August T. Noevere[1] and Craig S. Collier[2]
Collier Research Corporation, Newport News, VA, 23606

A tool has been developed to address the growing Design for Manufacturing needs for composite structures, specifically those manufactured with automated fiber placement. This manufacturing approach presents unique challenges associated with puckers and wrinkling, tow overlaps and gaps, fiber deviation, and laminate strength. Achieving a satisfactory laminate design usually requires finding compromises between those four areas. The developed tool, dubbed the Central Optimizer, assists with the process of balancing competing design metrics in automated fiber placement. This tool was developed under the NASA Advanced Composites Consortium with input from industry partners. Under this program, the Central Optimizer has been exercised on three different structures to verify its functionality and validate ability to improve the design process for automated fiber placement structures.

Nomenclature

C_i	=	Regression coefficient for i^{th} regression term
E_i	=	Exponent for i^{th} regression term
f	=	Regression function
KD	=	Strength allowable knockdown factor
P	=	Probability
R	=	Steering radius
t	=	Ply or laminate thickness
V_g	=	Gas volume fraction
θ_{dev}	=	Deviation of ply orientation from the rosette
$\theta_{new\ ref}$	=	Updated non-rosette reference direction for an element

Acronyms

ACC	Advanced Composites Consortium
AFP	Automated Fiber Placement
CAD	Computer Aided Drafting
CAPP	Computer Aided Process Planning
DFM	Design for Manufacturing
FEA	Finite Element Analysis
FEM	Finite Element Model
FOD	Foreign Object Debris
IFS	Inner Fixed Structure
NC	Numerical Controller

[1] Aerospace Research Engineer, Collier Research Corporation, Member AIAA
[2] President, Collier Research Corporation, Associate Member AIAA

NTL	Non-traditional laminate
PSS	Path Simulation Software
VCP	Vericut Composite Programming

I. Introduction

Design of Automated Fiber Placement (AFP) structures requires finding a balance between competing objectives in manufacturing, design, and stress analysis disciplines. Although this challenge is not new for aerospace structures, use of AFP introduces new constraints not found with metallic or composite hand-layup structures. AFP manufacturing consists of placing multiple continuous strips of unidirectional composite prepreg (known as tows) with a robotic head. The tow width for AFP typically ranges from 1/8" to 1". This manufacturing approach becomes particularly challenging on tool surfaces with complex curvature, as the tows tend to follow a "natural" path over the curvature. Often, these natural paths can cause fiber directions that may not necessarily align with requirements from the stress analysis (which is typically based on a 0/45/90 traditional laminate). Additionally, tow overlaps (also known as "laps") and gaps occur where tow paths converge due to the curvature of the tool surface.

This paper describes the development, functionality, verification, and validation of the Central Optimizer tool, which was created to address the challenges described. The Central Optimizer was developed under the NASA Advanced Composites Consortium (ACC) as a part of the Design For Manufacturing (DFM) software development task [1].

A. Motivation

Prior to the initiation of the DFM task, many design processes rely on conservative manufacturing assumptions made during stress analysis and design to ensure that the structural design will be manufacturable. For example, laminate material allowables for AFP composites often include strength reductions to account for the presence of laps and gaps in the laminate [2]. The Numerical Controller (NC) programmer, who is responsible for programming the AFP machines, is then required to generate laps and gaps at a rate less than what was used to derive the laminate strength allowables (communicated to the NC programmer as a manufacturing specification). The result is that the strength allowable reduction may be applied to the *entire* structure, instead of only regions that contain laps and gaps. This can cause the structural sizing to result in a laminate that is excessively thick, due to the reduced strength allowables. However, this process was necessary prior to the software development done in the DFM task to allow stress analysts to perform laminate sizing without having to rely on many lengthy iterations with NC programmers.

The presence of fiber angle deviation produces a similar challenge. In some scenarios, fiber angle deviation can cause a significant strength reduction in a laminate [3]. In others, deviation can actually improve the strength of the laminate, or simply have no effect. Determining the outcome requires mapping the as-manufactured fiber direction of every ply onto a Finite Element Model (FEM) and analyzing the result with each load case. Prior to the DFM task, the conservative approach was to include a laminate strength reduction according to the magnitude of the deviation (as determined by an NC programmer) in the panel being analyzed, regardless of whether or not the deviation would help or hurt the laminate strength (because this was unknown). This conservative assumption can also cause the structural weight to be higher than necessary.

In both scenarios described above, recurring theme is that lack of precise manufacturing information during stress analysis and design results in conservative assumptions made about AFP manufacturing, thus resulting in a structure that is heavier than necessary. The overarching goal of the software developed under the DFM task is to provide as much of the manufacturing data described above as possible to the stress analysis and design disciplines. Doing so allows for localized analyses to determine the true impact of AFP features, allowing for a more optimum AFP structure to be produced.

The objective of the DFM task was to develop and enhance software tools to provide an integrated design and analysis environment for AFP structures. Although there are several existing software tools dedicated to AFP manufacturing and also existing approaches for analyzing the strength of AFP structures, there is very little automation in the data exchanges between these two disciplines. Additionally, there was very little standardization of data formats in the data exchange between the two disciplines. This is primarily due to the fact that manufacturing data is usually in a CAD-based format, whereas structural analysis data is usually in a FEM-based format. The DFM task was focused on addressing these shortcomings to streamline the design process for AFP structures.

B. Literature Review

Several papers were written during the development of the Central Optimizer and associated software. Reference [4] describes the initial development of the data transfer capabilities between Vericut Composite Programming (VCP), an AFP Path Simulation Software (PSS), [5] and HyperSizer [6]. This data transfer included fiber directions and tow overlaps and gaps. Reference [7] provides an example of the application of this data transfer software to the design of an AFP Inner Fixed Structure (IFS) on a typical turbofan engine. The software was used to optimize the IFS laminates while accounting for the presence of fiber angle deviation and tow overlaps and gaps. Reference [8] describes further development of the Central Optimizer tool, including the software workflow and development of additional optimization tools. Reference [9] describes the final Central Optimizer software and presents an example optimization focused on minimizing the laminate deviations from a traditional 0/45/90° laminate.

C. CAPP Module

Another software developed in parallel to the Central Optimizer under the DFM task was the Computer Aided Process Planning (CAPP) Module. The CAPP module is focused on automating the tasks performed by a process planner to select AFP manufacturing parameters (such as machine speed, temperature, path generation, etc). The version of the CAPP developed during the ACC project was focused on selecting the path start point and layup strategy for each ply in a laminate. The use of this tool is described further in Section II.A.

D. AFP Challenges Addressed

From a manufacturing perspective, AFP defects must be minimized. Some defects such as tow twists, missing tows, Foreign Object Debris (FOD), and "shredders" (split/unraveled tows) are mostly related to the manufacturing process and can be corrected within the manufacturing discipline. However, there are also a variety of defects that can be precipitated by aggressive tow steering. These include defects such as puckers, wrinkles, and edge folds. An example of tow puckering is shown in Figure 1. These are of particular interest because tow steering is closely connected to the stress analysis discipline, as tow steering also influences the amount of fiber angle deviation in a laminate.

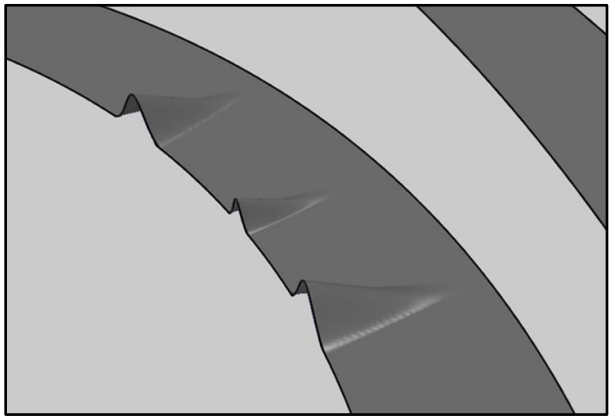

Figure 1. Example of puckering in a steered tow.

Additionally, fiber deviation from a traditional 0/45/90 laminate is a big concern for AFP structures with double curvature. If the structure has significant curvature, it can be challenging or impossible to generate tow paths that precisely follow 0/45/90 fiber orientations without generating excessive laps and gaps or AFP defects due to steering. Figure 2 demonstrates a "natural" fiber path (one without steering) over the tool surface of an IFS from a turbofan engine. At the two demonstrated start points, the fiber path is oriented perfectly at 45 degrees from the horizontal. However, the curvature of the surface forces the fiber paths to become significantly greater or significantly less than 45 degrees on the outer flange of the structure, depending on the placement of the start point.

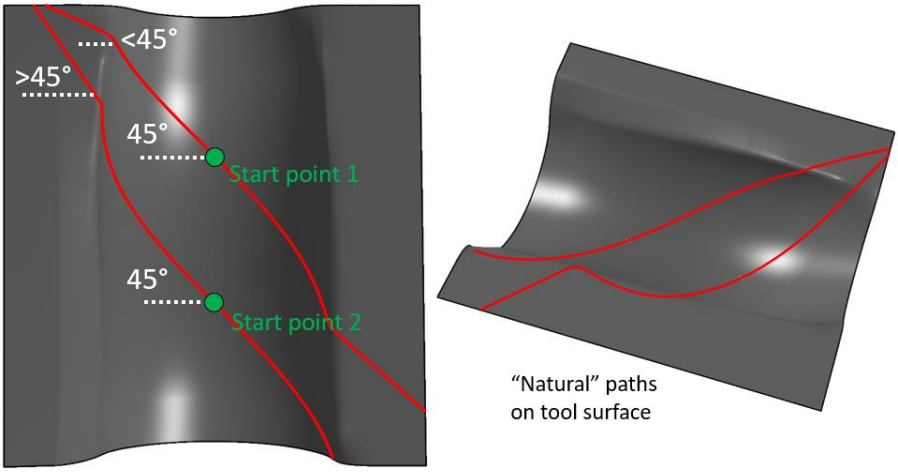

Figure 2. Impact of double curvature and start point on fiber angle deviation.

From a stress analysis perspective, the objective is to maintain the strength of the laminate to avoid failure with respect to loads derived from Finite Element Analysis (FEA). The most common composite analysis approach used by the commercial aviation industry is to evaluate laminate strains. One challenge that arises with AFP structures is that the fiber paths can deviate substantially from standard 0°, 45°, 90° orientations. This makes it difficult to make a valid comparison to the strain allowables derived for "traditional" laminates. However, including the fiber angle deviation in the strength tests of these Non-Traditional Laminates (NTLs) is also not usually viable because of the extremely high number of tests that would be needed to capture all the possible combinations of deviation through the thickness of the laminate. Thus, it is desirable to steer the tows to achieve as close to 0°, 45°, 90° orientations as possible.

Additionally, tow steering influences the formation of tow overlaps ("laps") and gaps which occur in locations where the tow paths converge or diverge. The gaps between tows essentially result in a hole in the ply, which can reduce the strength of the material. The laps and gaps can also stack on top of each other, causing the overall thickness of the laminate to deviate significantly, which is not ideal for bonded or fastened interfaces.

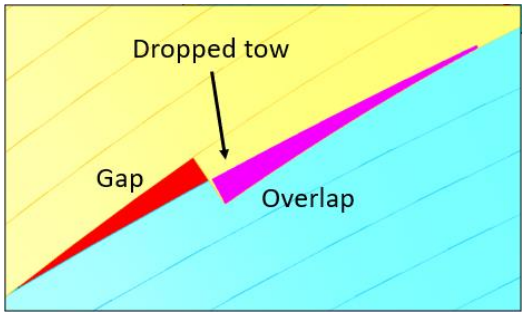

Figure 3. Example of tow overlaps and gaps in a path convergence zone.

The developed Central Optimizer tool is intended to help reconcile the competing objectives described above. The tool extracts data from manufacturing simulations and analyses, as well as stress analysis and laminate optimization, and overlays all relevant data. This approach improves the iterative process between the manufacturing, design, and stress analysis disciplines needed to find a satisfactory design.

E. Industry Partnership

The Central Optimizer tool has been developed by Collier Research as a part of the NASA Advanced Composite Consortium (ACC) in partnership with Aurora Flight Sciences, Boeing, NASA, Spirit Aerosystems, and the University of South Carolina McNair Center, all of which formed a Collaborative Research Team (CRT). These partners provided guidance on specific capabilities needed by the aerospace structures industry to enable a useful DFM tool for AFP structures.

Before any software was produced, the CRT first identified AFP defects of interest to the CRT to be addressed in the Central Optimizer. These defects were selected according to severity while also considering which AFP defects can actually be directly influenced by AFP process parameters. Some defects, such as Foreign Object Debris (FOD) are outside of the influence of the structural design itself, and therefore were not considered. The next step taken by the CRT was to define a software workflow and algorithms for the Central Optimizer, which are described in the next section. Next, the planned software capability was developed, followed by two rounds of evaluation and feedback from the CRT to plan future enhancements of the software. The evaluation, which includes software verification and validation, is described in Section III.

II. Methodology

The Central Optimizer tool provides data interfaces between multiple software in the manufacturing, design, and stress analysis disciplines. The tool is based in the HyperSizer software framework, which is a Finite Element Model (FEM)–based structural analysis and optimization tool. Data from manufacturing simulations can be imported and mapped to the FEM to be overlaid with stress analysis results. This allows informed decisions to be made for updating the laminate design, which can then be transferred back to the manufacturing tools.

A. Central Optimizer Workflow

The workflow for the Central Optimizer is depicted in Figure 4.

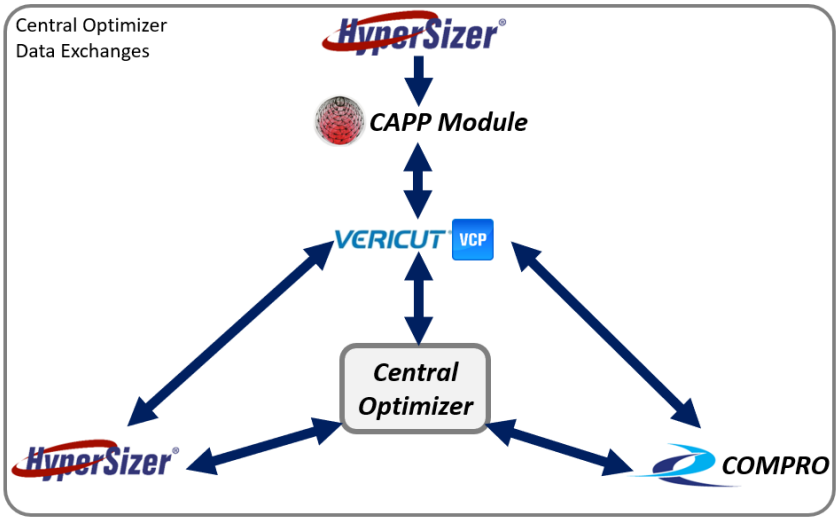

Figure 4. Workflow with the Central Optimizer.

The HyperSizer software performs the first step of the process by optimizing the laminates (both ply shapes and stacking sequence) to meet strength and stability requirements. Additionally, HyperSizer can perform a variety of custom analyses as analysis plugins. Several analysis plugins have also been developed and/or augmented under the ACC program for bonded joint analysis, two-bay crack analysis, post-buckling, Barely Visible Impact Damage (BVID) analysis, and Compression After Impact (CAI) analysis. An example of laminates optimized by HyperSizer are shown in Figure 5.

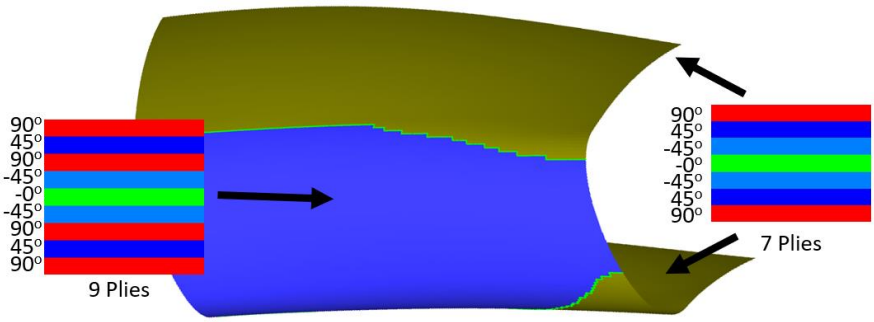

Figure 5. Example of laminates optimized by HyperSizer. 4]

Once the laminate optimization is performed in HyperSizer, the optimum plies are exported to manufacturing simulation tools. The first is the CAPP module. The CAPP determines optimum start points and layup strategies for each ply to maximize ply manufacturability. The "start point" for an AFP ply defines the seed point where all tow paths are propagated from. The "layup strategy" usually dictates how closely the tows follow a 0°, 45°, 90° orientation versus mitigating tow steering. Both are critical inputs to the manufacturing process planning.

Next, the plies are passed to VCP, which is used to define the tow paths over the structure to be placed by the AFP robot. VCP can calculate tow steering, angle deviation, and the presence of laps and gaps. All this data can then be mapped back to the FEM in HyperSizer for inclusion in the strength analysis. An example of the tow paths generated by VCP are shown in Figure 6.

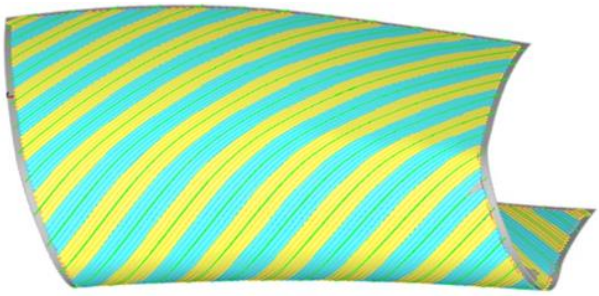

Figure 6. Example of tow paths on a complex contour tool.

The last step is to evaluate the probability of defect occurrence. This is done using physics-based simulations performed in the COMPRO [10] software. These simulations can predict the likelihood of defects that occur during AFP tape deposition, as well as cure defects such as porosity and wrinkling. The defect probability maps generated by these tools are also mapped back to the FEM in HyperSizer for inclusion in the analysis.

Finally, the Central Optimizer collects the metrics associated with each analysis and presents them to the user. This allows an informed decision to be made as to how the laminate design should be updated in the next design iteration. The Central Optimizer interface is shown in Figure 7.

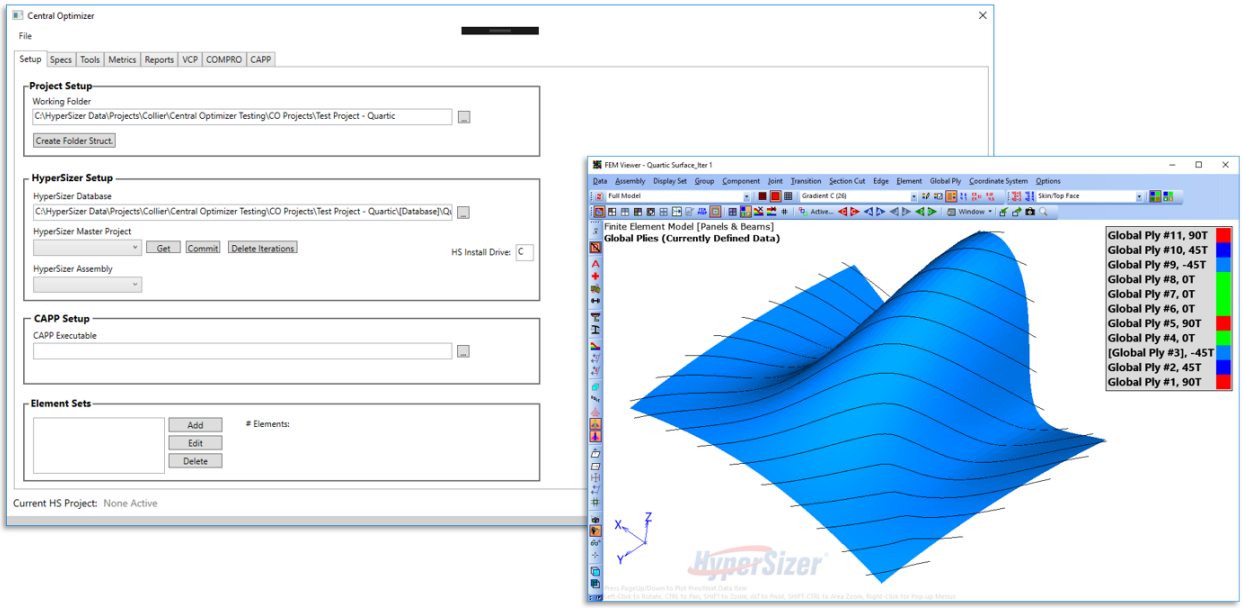

Figure 7. Central Optimizer interface.

B. Central Optimizer Tools

In addition to tracking the global design iterations for the AFP structure, the Central Optimizer contains a variety of tools to analyze the design and optimize AFP parameters. These are described in the sections below. Some of these capabilities have been described previously in Refs. [4], [7], [8], [9] and are simply summarized here.

1. *Mapping AFP Fiber Directions to FEM*

HyperSizer and the Central Optimizer are able to map fiber directions from VCP onto the FEM in HyperSizer. This is done with data output from VCP that provides the tangent vector to the fiber direction at the location of each element centroid for each ply. This mapping process has been described thoroughly in Ref. [4]. Figure 8 below shows an example of the mapping. This mapped data is then used to update the stress analysis as described in subsequent sections.

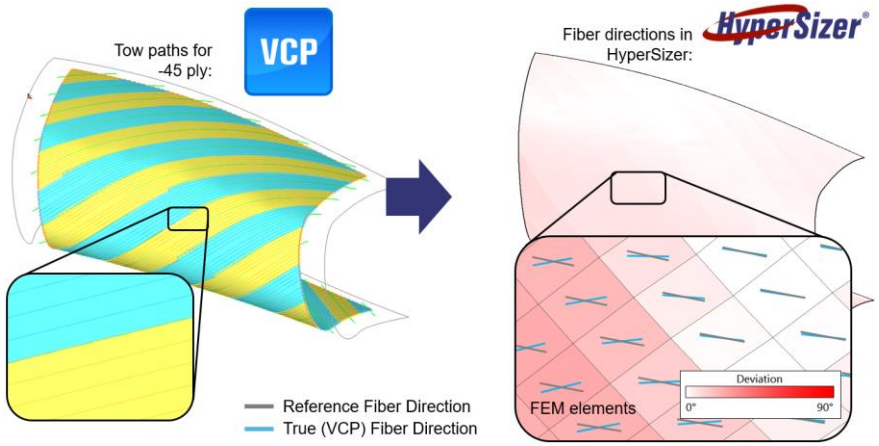

Figure 8. Example of mapping AFP fiber directions from VCP to HyperSizer [4].

2. *Mapping AFP Laps and Gaps to FEM*

HyperSizer and the Central Optimizer are also able to map laps and gaps predicted by VCP onto the FEM in HyperSizer. VCP outputs laps and gaps represented by a polyline around the perimeter of each feature. These polylines are then used to tesselate the features and map them onto the FEM. This mapping process is depicted in Figure 9. The result is that HyperSizer and the Central Optimizer then know which elements have laps or gaps on them in each ply, as well as the geometry (length, width, and area) of each feature.

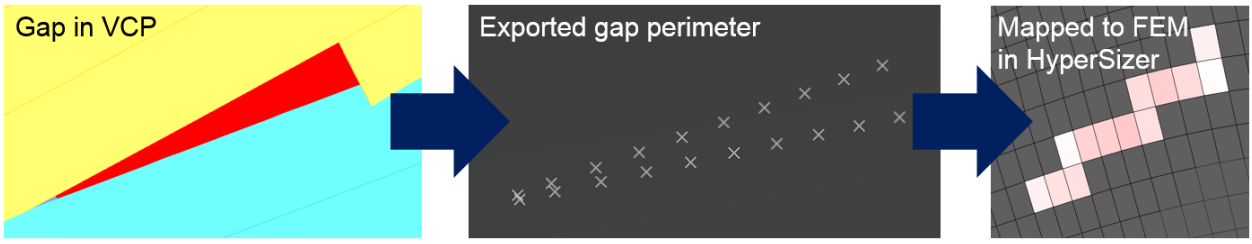

Figure 9. Process to map laps and gaps from VCP to HyperSizer [4].

The mapped lap and gap data are used to update the stress analysis as described in subsequent sections. Additionally, the mapped data is used to determine which elements on the FEM have missing or extra material due to the presence of accumulated laps or gaps. If multiple gaps from multiple plies coincide, they can cause the laminate to be thinner than intended in that location. An example of this data is shown in Figure 10.

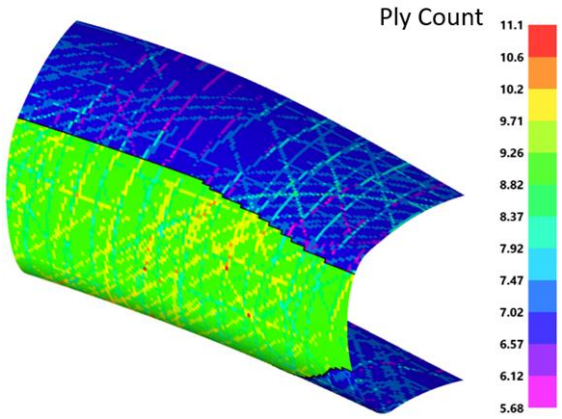

Figure 10. Ply count deviation due to lap and gap accumulation [8].

3. Iterate with FEA Including AFP Features

HyperSizer and the Central Optimizer are able to update the FEM with AFP data mapped from VCP. For NASTRAN FEMs, this is done by creating a unique FEM property for each element with AFP data. This allows a unique fiber orientation to be stored for each ply in each element. Additionally, having a unique FEM property allows ply thickness to be scaled in each element to account for the presence of laps and gaps.

4. Stress Analysis with Included AFP Features

The mapped AFP data described above is included in the HyperSizer stress analysis. The subsections below describe the approaches used for fiber directions and laps/gaps. The approaches accommodate both ply-based and laminate-based analyses.

4.1. Fiber Directions: Ply-Based Analysis

The ply-based analysis for composites in HyperSizer uses Classical Lamination Theory (CLT) to derive the stresses and strains in each ply in the laminate. CLT allows ply orientations to be defined at any arbitrary orientation, not just traditional 0/45/90 ply orientations. This lends itself well to using AFP fiber directions, which vary continuously across the elements in a structure. Additionally, there are no restrictions on most ply-based failure methods such as max stress, max strain, Tsai-Wu [12], Tsai-Hahn [11], etc. for use of non-traditional ply orientations.

4.2. Fiber Directions: Laminate-Based Analysis

Although the ply-based analysis described above is able to easily accommodate AFP fiber directions, this analysis approach is not commonly used by aircraft structure OEMs. Instead, a laminate-based analysis is often used because it simplifies the process of deriving material allowables. However, the majority of laminate-based failure analyses are not natively suited to handle any continuous fiber angle. Laminate-based failure usually consist of an allowable curve that is parameterized to describe the softness or hardness of the laminate. Examples of the parameter include %0°

plies, %45° plies, or the Angle Minus Load (AML) parameter. However, these allowable curves are constructed for laminates with only 0/45/90° ply orientations.

The most common approach to handling AFP fiber angle deviations is to apply a knockdown to the laminate allowable based on the severity of the deviations. This can be done either with an equation that describes the knockdown value as a function of deviation, or simply with knockdown "bins" based on deviation. For example, deviations <2° would have a knockdown of 1.0, deviations >2° and <5° would have a knockdown of 0.95, etc.

4.3. Laps and Gaps: Ply-Based Analysis

Similar to the ply-based analysis approach for fiber directions, this analysis utilizes an existing feature of CLT. Specifically, the thickness of individual plies can be varied in the laminate definition that is input to the CLT analysis. The thickness variation is determined by the size of the laps and gaps mapped to each element. The ply thickness is adjusted for the local presence of a lap or gap; laps add thickness and gaps remove thickness. If a gap covers 50% of the area of an element, then the thickness of the ply in that element is reduced by 50% [4]. These scaled ply thicknesses are input to the CLT analysis, which distributes stresses to plies accordingly.

4.4. Laps and Gaps: Laminate-Based Analysis

Two alternative approaches were taken to the laminate-based analysis for laps and gaps:

1) Gap width

   In this approach, strength knockdowns are determined by the width of gaps in elements. A user-defined knockdown curve is used to determine the value of the knockdown based on the widest gap in the element.

2) Laminate thickness reduction due to gaps

   In this approach, a thickness reduction scheme is used to calculate a reduced thickness for the laminate. This is very similar to the approach described in Section B.4.4 for ply thickness reduction, except that the thickness reduction of the entire laminate due to the presence of gaps is calculated for each element. The element knockdown factor is then determined from the equation shown below, where t_i is the original laminate thickness and t_{red} is the laminate thickness after accounting for the presence of gaps.

$$KD = \frac{t_{red}}{t_i} \tag{1}$$

5. Resize Laminates to Resolve Negative Strength Margins

After including AFP features in the stress analysis as described above, it is possible to find negative strength margins in the existing laminate design. An example of these strength margins is shown in Figure 11.

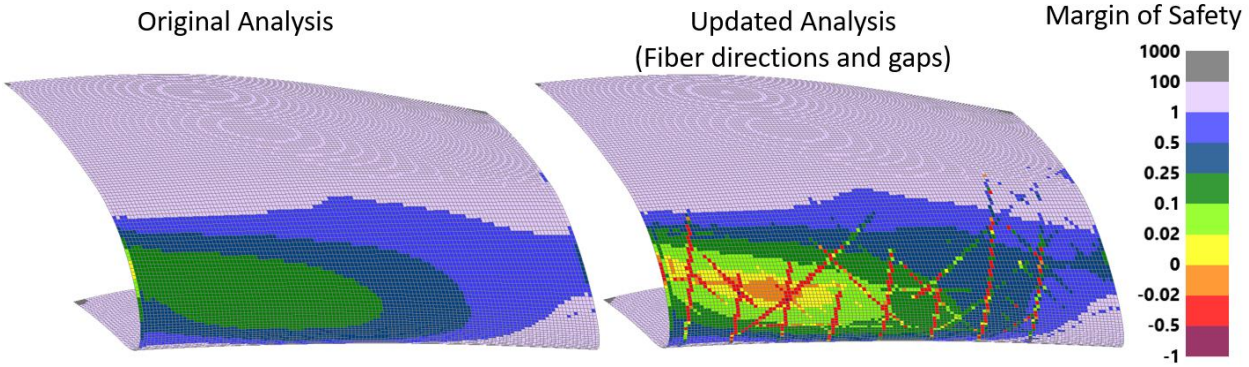

Figure 11. Laminate strength margins updated to include AFP data.

These negative margins must be resolved in the final design for the laminate. The challenge with resolving the negative margins is the feedback loop that exists between the VCP path simulation and the HyperSizer laminate optimization. Each time HyperSizer generates new plies, they must be run through VCP. Additionally, HyperSizer does not have the correct AFP data during optimization because the VCP simulation has yet to be run. The result is that neither

process can be correctly run without the output from the other process. To avoid this data feedback issue, the laminate optimization process in HyperSizer uses strength knockdowns based on the strength margins from the previous iteration where AFP data was included. Using these strength knockdowns causes HyperSizer to add plies or change the laminate stacking sequence to mitigate the detrimental impact of AFP features on laminate strength margins. The sizing knockdowns for AFP laminates (KD_{AFP}) are calculated as shown in Eq. (2). These values are calculated per-element from the margins of safety with AFP features, MS_{AFP}, and the original margins of safety, MS_{Ref}. An example of the resulting sizing knockdowns for fiber deviation is shown in Figure 12.

$$KD_{AFP} = \frac{MS_{AFP} + 1}{MS_{Ref} + 1} \tag{2}$$

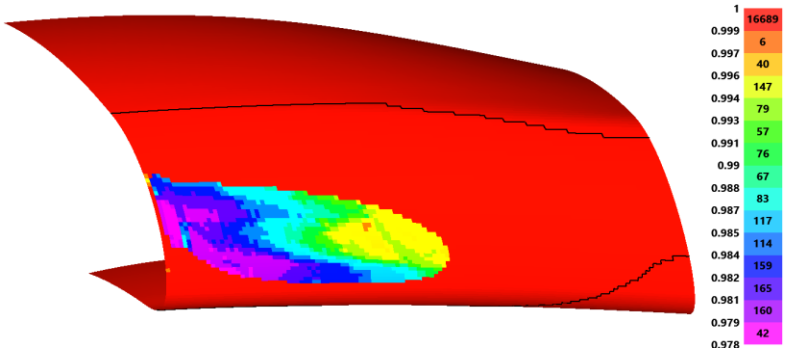

Figure 12. Sizing knockdowns from fiber deviation.

6. Analysis and Optimization of Through-Thickness Fiber Angle Deviation

Through-thickness angle deviation describes the *local* deviation from a traditional 0/45/90° laminate. A tool surface with complex curvature can have deviations that vary over the entire tool surface due to limitations in how much tows can be steered to achieve the desired fiber orientations. The laminate could have ply orientations at exactly 0/45/90° in one area, but with significant deviation in another area. The Central Optimizer is able to determine how much local deviation exists in each element. This requires the calculation of a unique reference direction $\theta_{new\ ref}$ for each element [7]. Equation (3) shows that this direction is calculated by the average of the min and max deviations of any ply in the laminate ($\theta_{dev,min,i}$ and $\theta_{dev,max,i}$).

$$\theta_{new\ ref,i} = \frac{\theta_{dev,min,i} + \theta_{dev,max,i}}{2} \tag{3}$$

The Central Optimizer also has the ability to optimize the ply orientations to minimize the through-thickness fiber angle deviation over the entirety of the part. The Central Optimizer explores varying each ply orientation individually and calculates an objective function value for each orientation explored. The objective function value is based statistical information about the deviations in all of the elements. Users can choose to minimize the maximum deviation value, the average, the 95th percentile value, etc. More detail and an example are provided in Ref. [7].

7. Surrogate Model for AFP Defects

The Central Optimizer includes an input for an AFP defects surrogate model to calculate the probability of AFP defects in each element. The probability is based on the steering radius values imported from VCP for each element in each ply. The equations below show the form of the surrogate model that can be input to the Central Optimizer. Figure 13 shows an example of calculated AFP defect probabilities.

$$f(R) = C_0 + C_1 \cdot R^{E_1} + C_2 \cdot R^{E_2} + \ C_i \cdot R^{E_i} \tag{4}$$

$$P(R) = 100 - \frac{100}{1 + e^{-f(R)}} \tag{5}$$

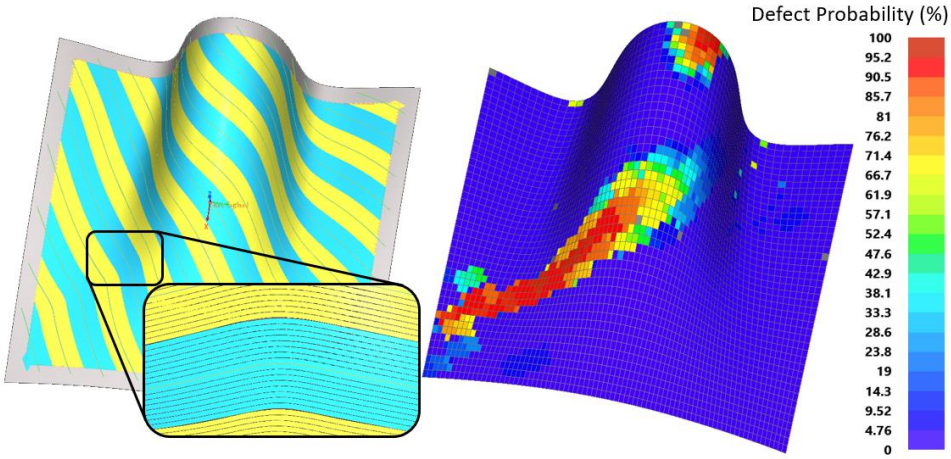

Figure 13. Calculation of AFP defect probability per element [7].

The data used to generate the surrogate model described above can be generated from either physical steering trials, or from trials done in the AFP defects simulation developed by Convergent Manufacturing Technologies US (CMTUS) and NASA in the COMPRO tool [13]. Future versions of the interface with this tool will allow for results from the AFP simulation to be mapped directly to the Central Optimizer instead of using a surrogate model.

8. Mapping Porosity from Cure Simulation

In addition to mapping AFP defects, the Central Optimizer can map locations of high porosity (measured as gas volume fraction V_g) from simulations of the laminate cure cycle. This simulation was also developed by CMTUS and NASA in the COMPRO tool [14]. The mapping approach used is to simply map values of V_g from the solid element mesh in COMPRO to the shell element mesh in HyperSizer using a mesh mapping routine in HyperSizer. Figure 14 below shows V_g from the cure simulation of a ply ramp with a caul plate. As expected, highest V_g and thus highest porosity is found at the base of the ply ramp where the upper surface of the laminate is concave. The caul plate is unable to fully conform to the concave area, and thus adequate pressure is not applied during cure. Figure 15 shows the same V_g values mapped to the shell element model in HyperSizer.

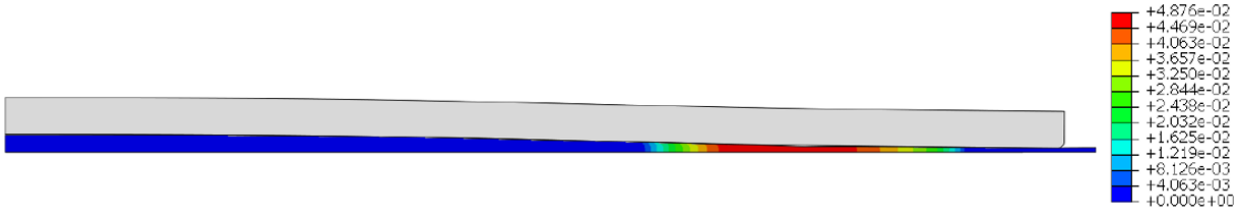

Figure 14. Gas volume fraction from cure simulation of ply ramp with caul plate [14].

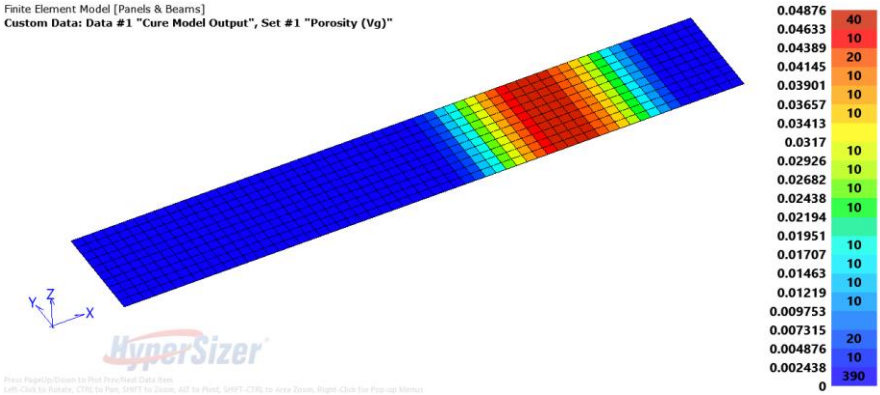

Figure 15. Gas volume fraction mapped to FEM in HyperSizer.

9. Design Metrics and Reports

One of the primary components of the Central Optimizer software is the ability to collect metrics for all aspects of the AFP laminate design in each design iteration. Additionally, the Central Optimizer generates detailed reports to accompany the design metrics. In each iteration of the design, the user reviews these metrics and reports to determine the steps needed to improve the design. Figure 16 shows an example of design metrics that would be collected after the initial iteration. The metrics are colored green or red according to whether they pass or fail the input specifications. Figure 17 shows an example of the reports that are produced corresponding to the strength margins. This data shows a breakdown of which plies cause negative margins, which margins are caused by laps and gaps, and which are caused by fiber angle deviation, the number of elements with negative margins and the area they cover, as well as several other diagnostic data points.

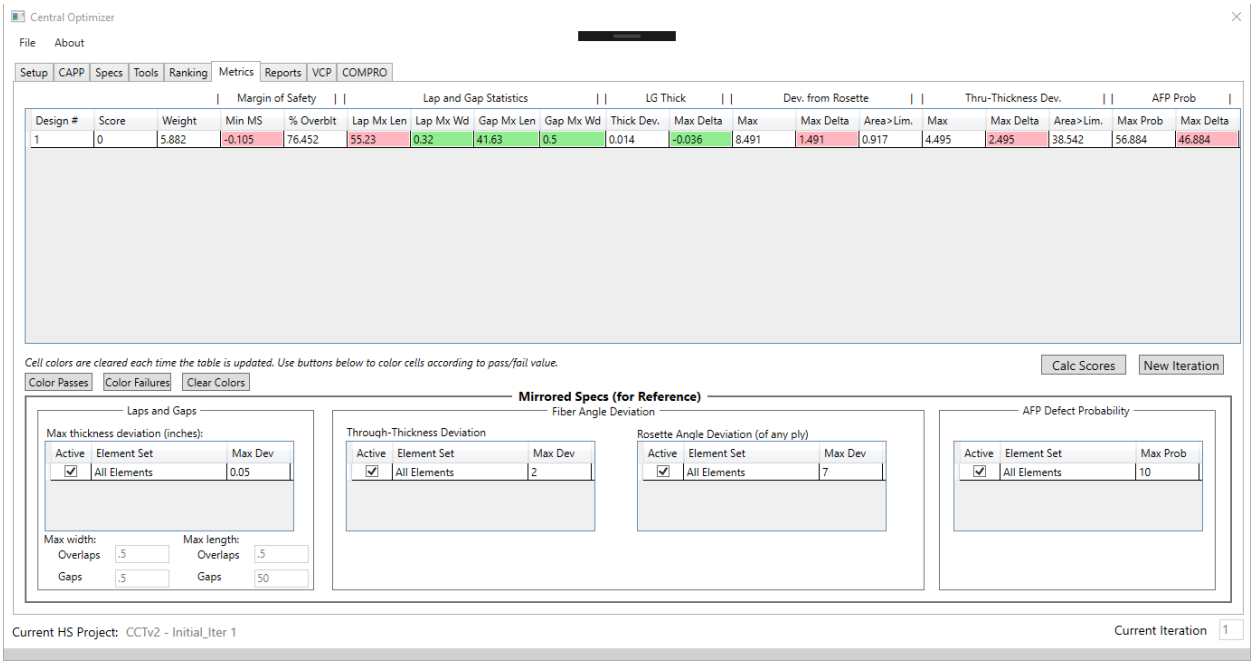

Figure 16. Design metrics tab in the Central Optimizer interface.

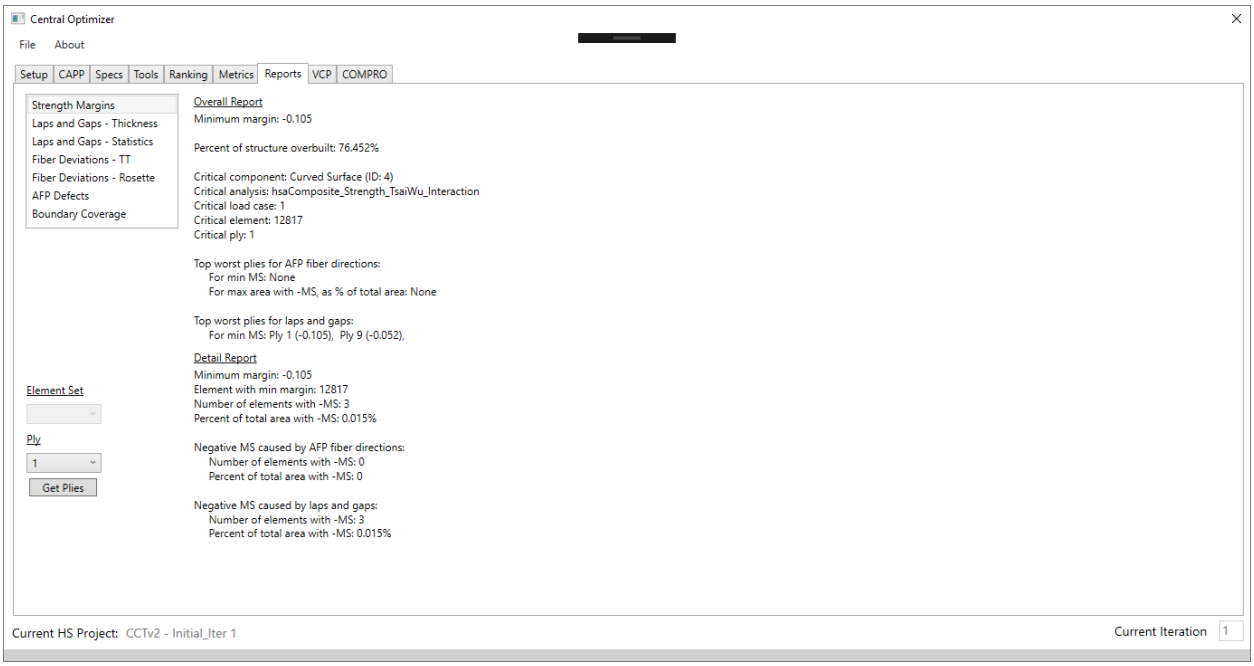

Figure 17. Reports tab in the Central Optimizer interface.

III. Verification and Validation

The Central Optimizer tool underwent verification and validation by industry partners on the ACC project. In these studies, the partners evaluated the effectiveness of the Central Optimizer compared to existing in-house tools and processes used to design AFP structures. This comprised of a mix of computer-only studies, as well as complete design, build, and test studies.

The first subsection below introduces the models used for verification and validation of the software. Next, the models are used to demonstrate the capabilities of the Central Optimizer, including mapping fiber directions, laps and gaps, AFP defects, etc. Not all capabilities are shown on all models for brevity. The final subsection summarizes the software evaluation.

A. Models used for Verification and Validation

This section describes the models that were used to verify and validate the Central Optimizer software. These models are intended to represent various parts of typical aerospace hardware. Each model includes CAD surfaces, FEMs with applied loads, and uses the IM7-8552 composite tape material, which was selected for the ACC project.

10. Saddle Geometry

This verification study was performed on a complex contour tool with a saddle shape. A variation of this geometry has been used extensively during the ACC program for AFP trials due to its challenging geometry. The verification performed with this tool did not include any builds, but the design process with the Central Optimizer was carried as if it were to be built. The geometry is shown in Figure 18.

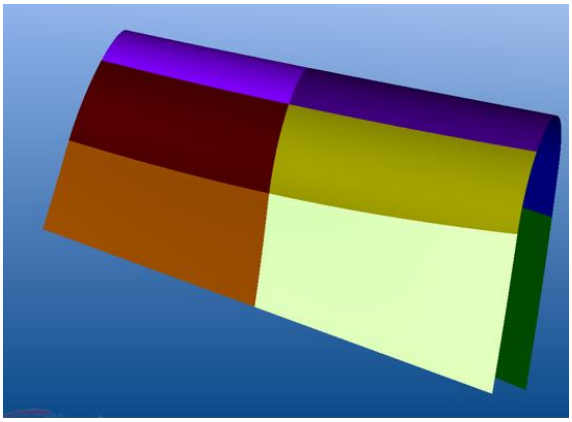

Figure 18. Saddle tool geometry.

11. Fuselage Panel

The validation study with the fuselage panel consisted of two builds: one with a design produced from existing AFP design tools and processes, and another with a design produced with the help of the Central Optimizer and associated software. The fuselage panel is a full-scale representation of a commercial aircraft forward fuselage section, including frames and stringers. The model geometry is shown in Figure 19.

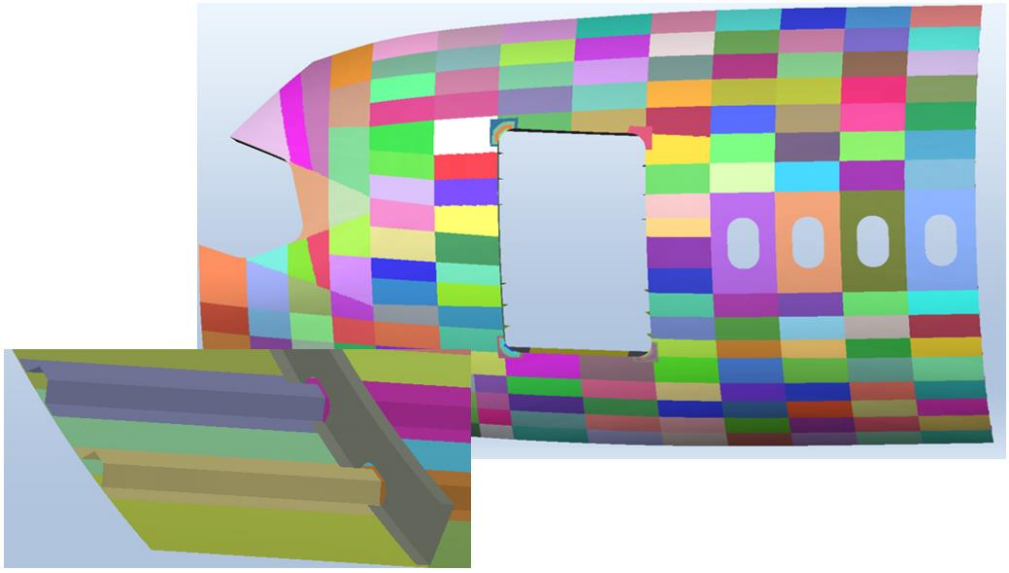

Figure 19. Fuselage model used in evaluation.

12. Wing Skin and Spar

The wing skin is a scaled version of that found in the NASA Common Research Model. A subsection of the upper wing skin and leading-edge spar were used, as shown in Figure 20.

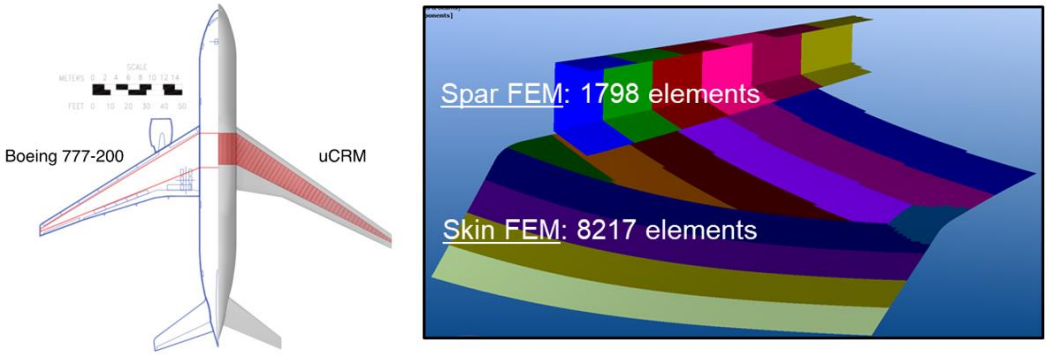

Figure 20. Wing skin and spar model used for software verification

B. Laminate Optimization with HyperSizer

Figure 21 shows an example of optimum plies that were generated by HyperSizer for the wing spar. HyperSizer uses internal FEA loads, strength and stability criteria, and ply stacking rules to come up with an optimum laminate for each panel. These laminates are then combined in a "sequencing" process to generate the final plies to be manufactured.

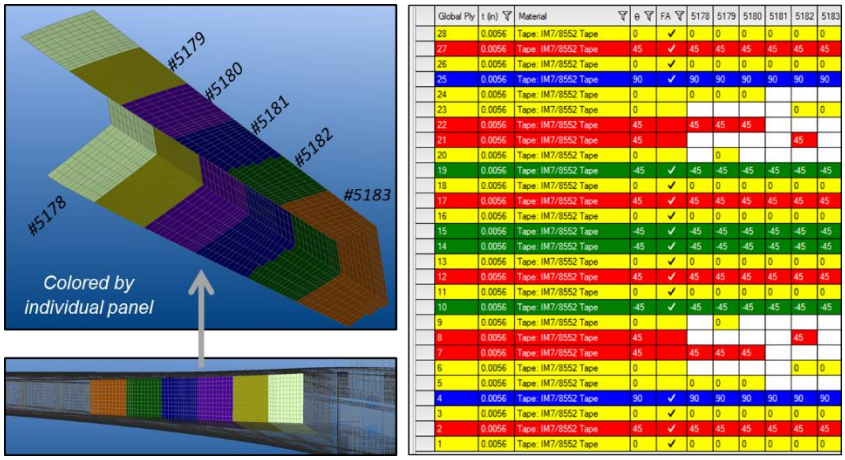

	Global Ply	t (in)	Material	θ	FA	5178	5179	5180	5181	5182	5183
	28	0.0056	Tape: IM7/8552 Tape	0	✓	0	0	0	0	0	0
	27	0.0056	Tape: IM7/8552 Tape	45	✓	45	45	45	45	45	45
	26	0.0056	Tape: IM7/8552 Tape	0	✓	0	0	0	0	0	0
	25	0.0056	Tape: IM7/8552 Tape	90	✓	90	90	90	90	90	90
	24	0.0056	Tape: IM7/8552 Tape	0		0	0	0			
	23	0.0056	Tape: IM7/8552 Tape	0						0	0
	22	0.0056	Tape: IM7/8552 Tape	45		45	45	45			
	21	0.0056	Tape: IM7/8552 Tape	45						45	
	20	0.0056	Tape: IM7/8552 Tape	0			0				
	19	0.0056	Tape: IM7/8552 Tape	-45	✓	-45	-45	-45	-45	-45	-45
	18	0.0056	Tape: IM7/8552 Tape	0	✓	0	0	0	0	0	0
	17	0.0056	Tape: IM7/8552 Tape	45	✓	45	45	45	45	45	45
	16	0.0056	Tape: IM7/8552 Tape	0	✓	0	0	0	0	0	0
	15	0.0056	Tape: IM7/8552 Tape	-45	✓	-45	-45	-45	-45	-45	-45
	14	0.0056	Tape: IM7/8552 Tape	-45	✓	-45	-45	-45	-45	-45	-45
	13	0.0056	Tape: IM7/8552 Tape	0	✓	0	0	0	0	0	0
	12	0.0056	Tape: IM7/8552 Tape	45	✓	45	45	45	45	45	45
	11	0.0056	Tape: IM7/8552 Tape	0	✓	0	0	0	0	0	0
	10	0.0056	Tape: IM7/8552 Tape	-45	✓	-45	-45	-45	-45	-45	-45
	9	0.0056	Tape: IM7/8552 Tape	0			0				
	8	0.0056	Tape: IM7/8552 Tape	45						45	
	7	0.0056	Tape: IM7/8552 Tape	45		45	45	45			
	6	0.0056	Tape: IM7/8552 Tape	0						0	0
	5	0.0056	Tape: IM7/8552 Tape	0		0	0	0			
	4	0.0056	Tape: IM7/8552 Tape	90	✓	90	90	90	90	90	90
	3	0.0056	Tape: IM7/8552 Tape	0	✓	0	0	0	0	0	0
	2	0.0056	Tape: IM7/8552 Tape	45	✓	45	45	45	45	45	45
	1	0.0056	Tape: IM7/8552 Tape	0	✓	0	0	0	0	0	0

Figure 21. Global plies generated by HyperSizer for the spar model.

C. Verification of AFP Fiber Direction Mapping

The process described in section II.1 was used to map fiber orientations from VCP to HyperSizer and the Central Optimizer for all three demonstration models. Figure 1 shows the rosette angle deviation for a 45° ply on the fuselage panel. Rosette paths were used exclusively on this panel, so the deviation is actually fairly low (within typical specs). The visible deviation is due to the finite width of the AFP courses, which causes the tows on the outside of the course to have some deviation. Additionally, the highest deviation occurs towards the nose of the fuselage panel where there is significant double curvature.

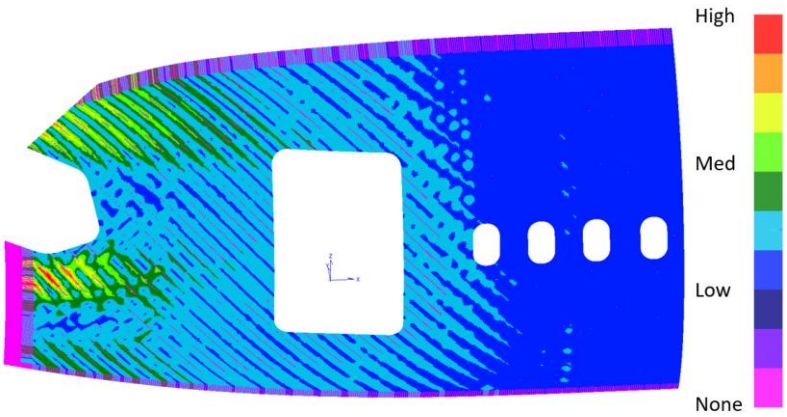

Figure 22. Fiber angle deviation for 45° ply on fuselage skin panel.

Figure 23 shows the deviation for a 0° ply on the saddle tool. This structure also primarily used rosette paths, resulting in fairly low deviation.

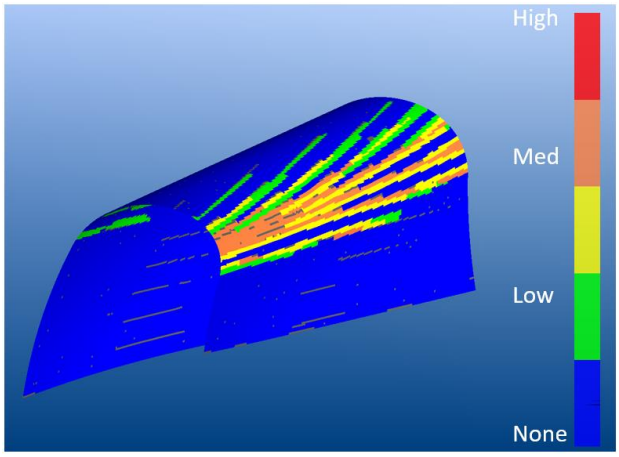

Figure 23. Fiber angle deviation for 0° on saddle tool geometry.

D. Verification of AFP Lap and Gap Mapping

The process described in II.2 was used to map laps and gaps from VCP to HyperSizer for all demonstration models. Figure 24 shows the gap width for a 0° ply on the fuselage skin panel. The majority of the gaps occur in the forward section of the fuselage, where there is double curvature. Since fiber angle deviation was low for this model, laps and gaps were the defect of interest.

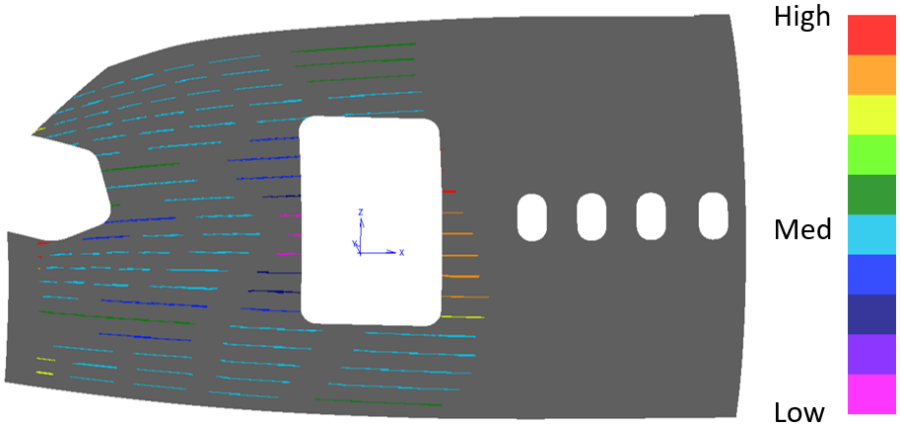

Figure 24. Gap width for 0° ply on fuselage skin panel.

Laminate strength knockdowns were generated once the gaps from all plies were mapped to the FEM. These knockdowns were used to resize the laminates. The knockdowns for the fuselage panel are shown in Figure 25. Although a significant portion of the structure has strength knockdowns less than 1.0, many of these were not actually problematic due to high strength margins that already existed in those locations. The only areas that were problematic (where negative strength margins occurred) were those that already had strength margins close to zero, or had coincident gaps from multiple plies. An example of the latter can be found below and to the left of the door cutout in Figure 25.

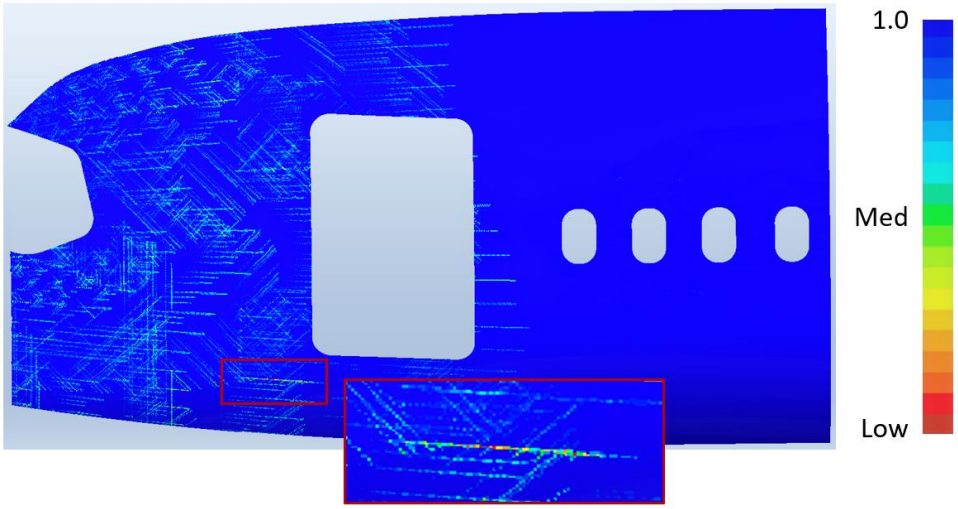

Figure 25. Laminate strength knockdowns due to gaps.

E. Verification of AFP Defect Probability

Figure 26 displays the steering radius values for a 45° ply along with the associated defect probabilities. The correlation between steering radius and defect probability is clear here in that smaller steering radii correspond to higher defect probability. This is the expected result and the feature is behaving as intended. This is a useful feature, but has one caveat in that, like other tools, is only as good as the input data, or model. The surrogate model is a good compromise for the near term, but requires physical test data, which may not be available or feasible to obtain for every project. The ideal goal would be to use the physics-based simulation as described in Section B.7, but that was not a possibility at this time. A better understanding of wrinkle probability is a critical goal and the Central Optimizer is making progress in making this obtainable. Additional physical testing is required to validate the surrogate model correlations. As this was purely a software validation, the accuracy of the defect prediction could not be evaluated, but the software tools and all data transfer and visualization functioned as expected.

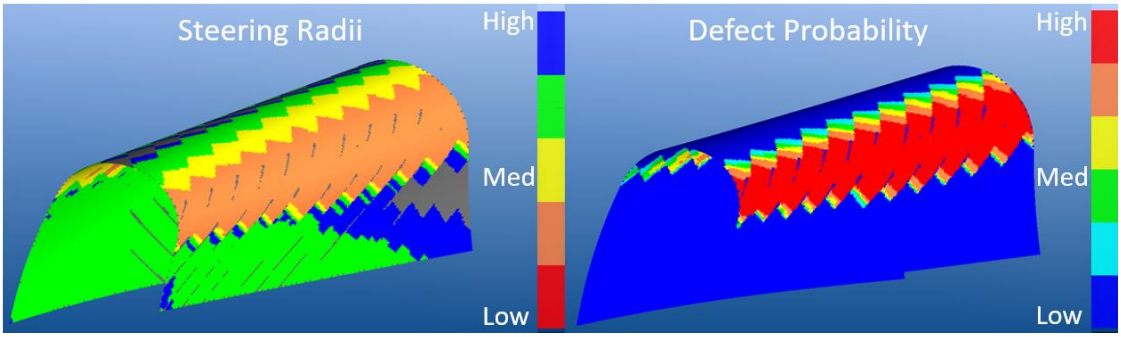

Figure 26. Per-element steering radii and defect probability on the saddle tool.

A similar calculation was performed on the fuselage panel. Figure 27 shows the steering radii mapped from VCP and defect probability calculated by the Central Optimizer. Once again, the nose area shows the most activity due to the double curvature in this region. The areas of low steering radii match up with the areas of high calculated defect

probability. Also, it is interesting to note that the areas of higher defect probability match up with the locations of recorded defects (Figure 29) in the optimized validation build.

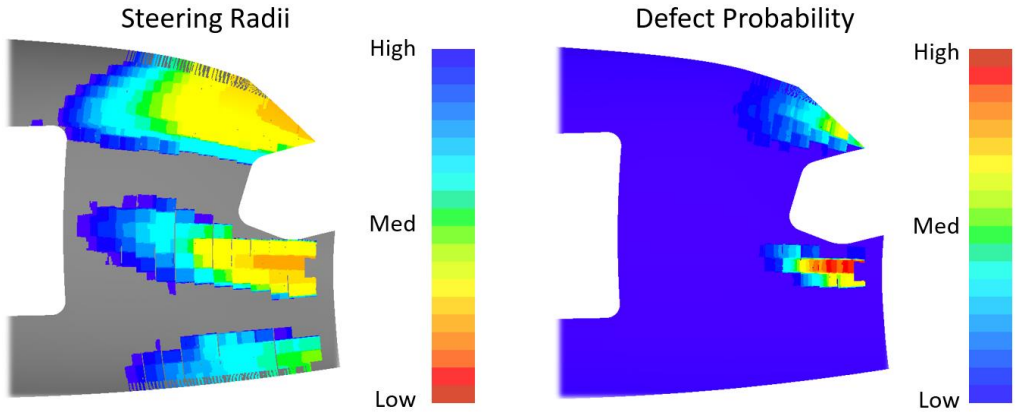

Figure 27. Per-element steering radii and defect probability on the fuselage panel for 90° ply.

F. Verification of Through-Thickness Angle Deviation Optimization

As described in section II.6, the Central Optimizer can analyze angle deviation and also optimize this deviation to lessen the effect across the laminate as a whole. The idea is that nominal ply orientations can be adjusted to lessen the extreme deviations by "smoothing" out the overall deviation across the ply. The Central Optimizer successfully optimized the angle deviations for this trial and the results for the saddle tool can be viewed below in Figure 28. The key takeaway from this image is that the areas of highest deviation (orange) were lessened by shifting the nominal ply orientations. This in turn created more minor deviations (green), but the overall specification violations were less. This is considered one of the most useful features of the Central Optimizer and provides designers and NC programmers with a valuable tool to better understand the through-thickness effects of angle deviation and attempt to correct specification-violating errors.

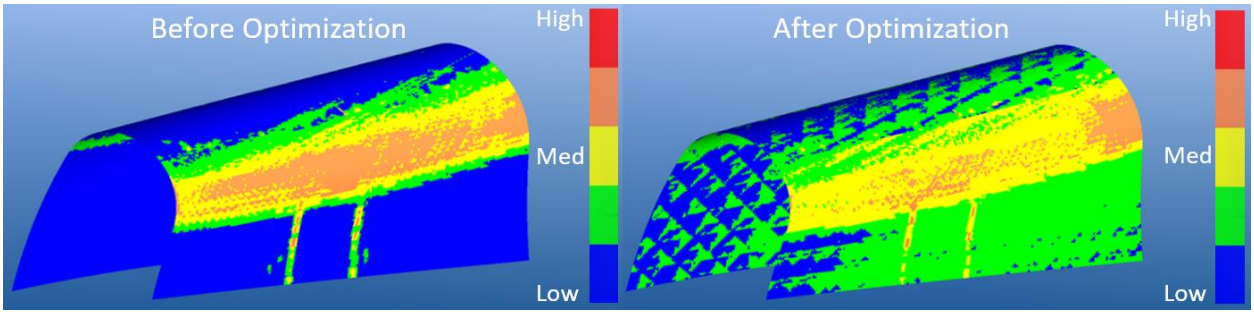

Figure 28. Through-thickness fiber angle deviations before and after optimization.

G. Validation Builds

In addition to the software verification performed above, two validation builds were performed for the fuselage panel to determine the impact on AFP defects after considering all of the analyses described above. The first build was the "baseline," using existing capabilities to design the fuselage panel. The second build was the "optimized" build using some of the software tools described above to generate the design. Figure 29 shows the comparison of recorded AFP defects between the baseline and optimized build. There was a clear reduction in the number of defects between the two builds.

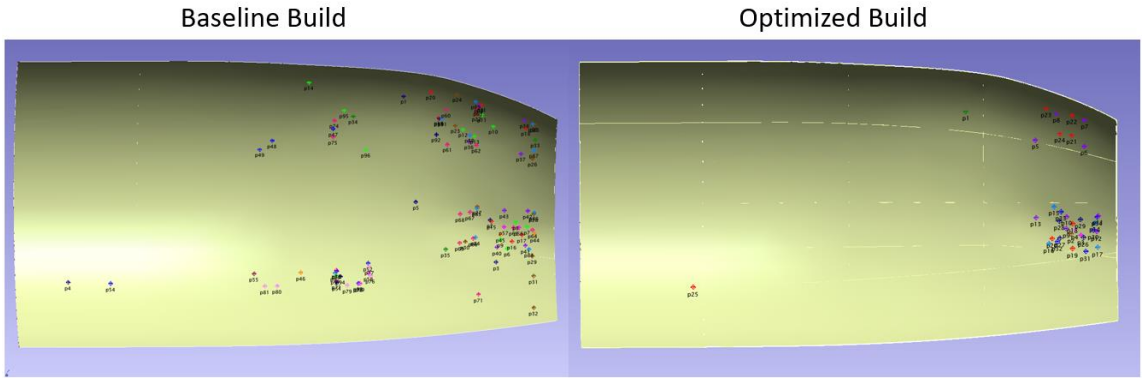

Figure 29. AFP defect locations from baseline and optimized build.

H. Software Evaluation Summary

The interactive software evaluation and feedback performed by the industry partners in the DFM task was highly productive. The feedback helped the software development team immediately identify areas for improvement in the software. As the Central Optimizer software is still in a prototype phase, it was expected that many iterative updates would be needed to prepare the software for full deployment on a structural design program. The data collected during the evaluation was used to plan out the next version of the Central Optimizer, as described in the next section.

The final results of the evaluation studies were not as clear-cut as originally anticipated, primarily due to the challenges of developing and deploying an entirely new software package within a three-year project. Two of the primary metrics considered were structural weight and design cycle time with and without the Central Optimizer. The latter was found to be very hard to quantify due to the time it took engineers to learn the new Central Optimizer software, as well as debugging that was performed at the initial deployment. The only recorded datapoint was for the wing skin structure optimization, with a labor savings of 59%.

The delta in weight between the baseline and optimized structures varied depending on the chosen analysis approach. The optimized wing skin structure was found to be 8.7% lighter. For the saddle tool, two different optimization approaches were taken, resulting in weights 4.05% and 25.1% heavier than the baseline. However, in this optimization, the way in which the AFP defects were analyzed could only cause the weight to increase because no strength benefits were allowed from the presence of tow overlaps. Since the baseline design did not include defect analysis, the weight could only increase, not decrease. Additionally, more investigation is needed for the second optimization data point to identify if appropriate strength knockdowns were applied for the AFP gaps. For the fuselage panel, the optimization resulted in a weight 13.8% higher than baseline, again due to selected analysis approach. Further work is needed to generate a comparable weight.

IV. Conclusion

Despite the challenges described above, the Central Optimizer was able to achieve the primary goal of interfacing stress analysis/sizing and AFP manufacturing to provide a software environment where engineers can simultaneously consider the constraints and performance in both disciplines. The industry partners were able to execute the majority of the new capabilities as intended. The data collected during the software verification and validation proved to be very valuable to plan enhancements to realize the full potential of the Central Optimizer.

One key area for improvement is to further streamline the coupling between stress analysis and AFP path simulation. The current data transfer process as described in this paper requires several manual button-clicks to pass the AFP data from VCP to HyperSizer. Fully automating this data transfer would allow for more thorough optimization because many different AFP paths could be simultaneously explored. Additionally, automation would remove the requirement for the stress analyst to learn how to use VCP, thus reducing the learning curve for the tool.

Another area to improve is the stress analysis of AFP data by developing approaches that allow for accurate analysis of as-manufactured structures instead of conservative “worst case” blanket knockdowns applied to material strength allowables. This would allow for full utilization of the manufacturing data that is mapped to HyperSizer by the Central Optimizer because the structure would be thickened only in areas with defects and high internal loads. These analysis

approaches are current topic [15] relevant to many researchers in the composites field and will be incorporated into the Central Optimizer as they gain adoption by industry.

The Central Optimizer will continue to be enhanced with capabilities described above to further pursue the goals of creating a DFM tool for AFP structures.

Acknowledgments

The material is based upon work supported by NASA under Award Nos. NNL09AA00A and 80LARC17C0004.

This work was heavily supported by fellow team members of the 2C22 Design for Manufacturing task in the NASA Advanced Composites Consortium. The team included Gary Wolfe of Aurora Flight Sciences; Jeron Moore, Sayata Ghose, Bill Avery, and Brice Johnson of the Boeing Company; Brian Grimsley of NASA Langley Research Center (task lead); Trevor Angell, Jared Ross, Ruth Ross, Ben Ferrell, and Steve Oyarzabal of Spirit Aerosystems; and Ramy Harik and Joshua Halbritter of the University of South Carolina.

References

[1] Warwick, G., "NASA Project Seeks Faster Certification of Composites." Aviation Week, November 2017. Accessed Dec 2019. https://aviationweek.com/technology/nasa-project-seeks-faster-certification-composites

[2] Li, X., Hallett, S. R., Wisnom, M. R., "Modelling the Effect of Gaps and Overlaps in Automated Fiber Placement (AFP) Manufactured Laminates," *Science and Engineering of Composite Materials*, Vol 22, No. 2, 2015, pp. 115-129.

[3] Yang, X., Nanni, A., Haug, S., Sun, C. L., "Strength and Modulus Degradation of CFRP Laminates from Fiber Misalignment," *Journal of Materials in Civil Engineering, ASCE*, 2002

[4] Noevere, A., Collier, C., "Mapping Manufacturing Data for Stress Analysis of Automated Fiber Placement Structures." *2018 AIAA/ASCE/AHS/ASC Structures, Structural Dynamics, and Materials Conference*, Kissimmee, FL, 2018, https://doi.org/10.2514/6.2018-0228

[5] Vericut Composite Programming, Software Package, Ver. 8.1, CGTech, Irvine, CA, 2019.

[6] HyperSizer, Software Package, Ver. 7.3, Collier Research Corporation, Newport News, VA, 2019.

[7] Noevere, A., Collier, C., "Integrated AFP Manufacturing and Stress Analysis/Design Process." *2018 American Society of Composites Technical Conference*, Seattle, WA, 2018

[8] Noevere, A., Collier, C., "Development of a Design for Manufacturing Tool for Automated Fiber Placement Structures." *2019 AIAA/ASCE/AHS/ASC Structures, Structural Dynamics, and Materials Conference*, San Diego, CA, 2019, https://doi.org/10.2514/6.2019-0520

[9] Noevere, A., Collier, C., Harik, R., Halbritter, J., "Development of a Design for Manufacturing Tool for Automated Fiber Placement Structures." *2019 AIAA/ASCE/AHS/ASC Structures, Structural Dynamics, and Materials Conference*, San Diego, CA, 201, https://doi.org/10.2514/6.2019-0520

[10] COMPRO, Software Package, Convergent, Vancouver, BC, Canada, 2018

[11] Tsai, S., & Hahn, H. (1980). Introduction to Composite Materials. Lancaster: Technomic Publishing Company.

[12] Tsai, S., & Wu, E. (1971). A General Theory of Strength for Anisotropic Materials. Journal of Composite Materials, 58-80.

[13] Forghani, A., Hickmott, C., Hutten, V., Bedayat, H., Wohl, C., Grimsley, B., Coxon, B., Poursartip, A., Experimental Calibration of a Numerical Model of Prepreg Tack for Predicting AFP Process Related Defects, *SAMPE 2018 Technical Conference and Exhibition*, Long Beach, CA, 2018

[14] Bedayat, H., Forghani, A., Hickmott, C., Palmieri, F., Grimsley, B., Coxon, B., Fernlund, G., Poursartip, A., Numerical and Experimental Study of Local Resin Pressure for the Manufacturing of Composite Structures and their Effect on Porosity, SAMPE 2018 Technical Conference and Exhibition, Long Beach, CA, 2018

[15] Rhead, A., Dodwell, T., "The effect of tow gaps on compression after impact strength of robotically laminated structures," *Computers, Materials and Continua*, 2013